Talanta 83 (2011) 1074–1078

Contents lists available at ScienceDirect

Talanta

journal homepage: www.elsevier.com/locate/talanta

Estimation of chromatographic peak shape parameters in Fourier domain

Attila Felinger*

Department of Analytical and Environmental Chemistry, University of Pécs, Ifjúság útja 6, H–7624 Pécs, Hungary

ARTICLE INFO

Article history:
Available online 8 October 2010

Keywords:
Fourier transform
Hartley transform
Curve fitting
Chromatography

ABSTRACT

A number of models in chromatography have analytical solutions in the Laplace or Fourier domain. Often, the moments of the Laplace domain solutions are calculated to characterize the peak shape. Nonlinear fitting in the Fourier domain can be performed to exploit the entire peak shape rather than the moments only. Curve fitting in the Fourier domain offers an attractive alternative for parameter estimation. In this study we will show – with some simple applications – the possibilities of estimation of chromatographic peak shape parameters in Fourier domain. Various models are fitted to different transient signals.

1. Introduction

Fourier methods have been very popular in analytical chemistry. Fourier transform proved to be a rather powerful means in various methods of signal and resolution enhancement [1]. Noise filtering with a variety of smoothing windows can be carried out more effectively in Fourier domain than with moving window averaging in time domain, although the two approaches are equivalent in theory. Fourier-domain filtering is mostly used as a low-pass filter, i.e. to cut-off the high-frequency region of the Fourier transform by an appropriate smoothing window [2].

Deconvolution of the instrumental broadening effects can also be rather easily carried out via the Fourier transform of the signal. The deconvolution of overlapping peaks by frequency domain deconvolution consists in calculating the Fourier transform of the chromatogram, dividing it with the Fourier transform of an appropriate sharpening function followed by taking the inverse Fourier transform. The broadening of a chromatographic band is influenced by several on-column and extra-column factors. The band broadening of the peak is simply characterized by the variance of the peak, because the variances of the individual processes – due to injection, detector, tubing, column, etc. – are additive. Thus, the various band broadening and distorting effects can be deconvoluted as long as the behavior of the system is linear [3–5].

A statistical approach for extracting average properties of multicomponent chromatograms has been developed by Fourier analysis or power spectrum analysis [6–10]. The aim of the power spectrum analysis is to determine the number of detectable components, the mean peak width, and the retention pattern. The Fourier analysis regards the chromatogram as a finite-length fraction of a stochastic process. Fourier analysis can be applied to ordered or disordered chromatograms as well and the repetitive occurrences of peak clusters can be identified to estimate the number of components or chemical families.

The estimation of the peak shape parameters can be performed in frequency domain also [11]. There is a two-fold advantage of doing that. First, the high-frequency noise is eliminated by the Fourier transformation of the signal and, secondly, one can observe in which region of the frequency domain is the important information contained. Felinger et al. used the extended Kalman filter to recursively estimate the peak shape parameters of noisy chromatograms.

Several models of chromatography offer simple solutions in the Laplace and the Fourier domain; very often the inverse transformation of the solution of the model to time domain is quite complicated, in some cases no analytical solution of the inverse transform exist. In those cases, when the time domain expressions of a model are not readily available, parameter estimation in the Fourier domain offers an attractive alternative for direct determination of model parameters [12]. In this study we will show – via some direct applications – the possibilities of the estimation of the chromatographic peak shape parameters in Fourier domain.

2. Theory

2.1. Fourier transform

The Fourier transform of a continuous function $f(t)$ is defined by the following integral:

$$F(\omega) = \int_{-\infty}^{\infty} f(t)e^{-i\omega t}\,\mathrm{d}t = \int_{-\infty}^{\infty} f(t)(\cos\omega t - i\sin\omega t)\,\mathrm{d}t \qquad (1)$$

where t is time, ω is frequency and i is the imaginary unit.

* Fax: +36 72 501 518.
E-mail address: felinger@ttk.pte.hu.

0039-9140/$ – see front matter © 2010 Elsevier B.V. All rights reserved.
doi:10.1016/j.talanta.2010.10.001

The Fourier transform of a digitized signal – containing N data points recorded over a time period T with $\Delta t = T/N$ sampling time – can be calculated with discrete Fourier transform as

$$F_n = \frac{1}{N}\sum_{k=0}^{N-1} f_k e^{-i2\pi nk/N}, \quad n = 0, 1, \ldots, N-1 \tag{2}$$

The frequency ω_n that belongs to value F_n is

$$\omega_n = \frac{2\pi n}{T} = \frac{2\pi n}{N\Delta t} \tag{3}$$

The distance between adjacent harmonics is determined by the observation time T

$$\Delta\omega = \frac{2\pi}{T} \tag{4}$$

The maximum observable angular frequency depends on the frequency of data acquisition:

$$\omega_{\max} = \frac{\pi N}{T} = \frac{\pi}{\Delta t} \tag{5}$$

When the Fourier transform of a signal containing N points is calculated by an FFT algorithm, the result is a complex array containing N real (X_r) and imaginary (X_i) values. The data array is, however, redundant, because the second half of the array is the mirror image of the first half. The first element of the real part $X_{r,1}$ contains the area or the mean of the time-domain signal, depending on the algorithm. The first element of the imaginary part $X_{i,1}$ is always zero when a real function is being transformed. The second element of either array contains the data for frequency $\omega = 2\pi/T$, etc. The $(N/2+1)$ th element belongs to $\omega_{\max}$. The further points of the arrays contain the Fourier spectrum for negative frequencies.

2.1.1. Convolution theorem

The convolution theorem is the most powerful Fourier theorem used in signal processing. The convolution integral of two functions is defined as

$$h(t) = \int_{-\infty}^{\infty} f(u)g(t-u)\,\mathrm{d}u \tag{6}$$

According to the convolution theorem of the Fourier transform, the convolution integral in time domain simplifies to a multiplication in frequency domain

$$f(t) * g(t) \Leftrightarrow F(\omega)G(\omega) \tag{7}$$

where operator $*$ stands for convolution.

2.2. Hartley transform

The Hartley transform is closely related to the Fourier transform. The Hartley transform of a time-dependent signal, $h(t)$, is defined as[13]

$$H(\omega) = \int_{-\infty}^{\infty} f(t)(\cos\omega t + \sin\omega t)\,\mathrm{d}t \tag{8}$$

The major difference between Fourier and Hartley transforms is that $H(\omega)$ is a real function, as opposed to the complex Fourier transformed signal. There exists a simple connection between the Fourier, $F(\omega)$, and the Hartley, $H(\omega)$, transform of a signal: the Hartley transform is obtained when the imaginary part of the Fourier transform is subtracted from its real part

$$H(\omega) = \Re F(\omega) - \Im F(\omega) \tag{9}$$

The linearity, shift, convolution, derivative, etc. properties of Fourier transform hold true for Hartley transform too.

The Hartley transform in sparsely utilized in analytical chemistry. Economou et al. for instance, used the fast Hartley transform for the deconvolution of overlapping peaks [14].

3. Experimental

An Agilent 1100 liquid chromatograph – equipped with a multisolvent delivery system, a manual sample injector with a 20-μL loop, a column thermostat, a multi-wavelength UV detector and a Chemstation software – was used for all measurements. The column used was a Waters Symmetry C_{18} column (4.6 mm × 75 mm, average particle size 3.5 μm). Phenol and thiourea were purchased from Sigma–Aldrich; J.T. Baker HPLC grade methanol and Milli-Q ultra pure water was used at all experiments.

The flow rate was 0.50 mL/min. The column thermostat was set at 20 °C. Each measurement was executed with methanol–water (80:20, v/v) solution as mobile phase. The standard mixture contained 0.8 μg/mL of phenol and 1.6 μg/mL thiourea. 20 μL of the standard mixture was injected in all measurements. The components were detected at 254 nm. The data acquisition frequency was 20 Hz.

3.1. Computations

Calculations (time domain and frequency domain curve fitting) were carried out by the public domain *gnuplot* software. That software utilizes the Levenberg–Marquardt algorithm for nonlinear least-squares fitting. The nonlinear fitting procedure was carried out on the raw chromatographic data or on the Fourier transformed data without additional noise filtering.

4. Results and discussion

4.1. Injection without the column

When we remove the column from the instrument and directly connect the injector to the detector, we record a band profile that characterizes the extra-column contribution of the HPLC instrument. In most of the cases – provided that the injected volume is small – the exponentially modified Gaussian (EMG) peak fits well that peak. The EMG peak is obtained with the convolution of a Gaussian and exponential decay function [1]:

$$f(t) = \frac{1}{2\tau}\,\exp\left[\frac{\sigma^2}{2\tau^2} - \frac{t-m}{\tau}\right]\,\mathrm{erfc}\left[\frac{\sigma}{\sqrt{2}\tau} - \frac{t-m}{\sqrt{2}\sigma}\right] \tag{10}$$

where m is the mean, σ is the standard deviation of the Gaussian peak, τ is the time constant of the exponential decay function.

The Fourier transform of the EMG function is [5,11]

$$F(\omega) = \frac{e^{-\omega^2\sigma^2/2 - i\omega m}}{1 - i\omega\tau} \tag{11}$$

The real and imaginary parts of $F(\omega)$ are, respectively

$$\Re F(\omega) = e^{-\omega^2\sigma^2/2}\frac{\cos\omega m + \omega\tau\,\sin\omega m}{1+\tau^2\omega^2} \tag{12}$$

and

$$\Im F(\omega) = -e^{-\omega^2\sigma^2/2}\frac{\omega\tau\,\cos\omega m - \sin\omega m}{1+\tau^2\omega^2} \tag{13}$$

The Hartley transform of the EMG model is

$$H(\omega) = e^{-\omega^2\sigma^2/2}\frac{(1-\omega\tau)\cos\omega m + (1+\omega\tau)\sin\omega m}{1+\tau^2\omega^2} \tag{14}$$

When the EMG model is fitted to experimental data, the conventional time domain fitting is probably more straightforward than the fitting in Fourier or Hartley domain. The real advantage of the

fitting procedure in frequency domain lies in the ability to exploit models that do not have a closed analytical form in time domain. The EMG function, however, can serve as a reference model that can equally be fitted in both time and frequency domains. A comparison of the numerical values of the parameters obtained by various fitting procedures can help judge whether or not the parameter estimation is biased.

To determine the extra-column contribution of the instrument, thiourea was injected into a mobile phase containing 80:20 % (v/v) methanol–water. The recorded signal is plotted in Fig. 1a. When we fit Eq. (10) to the recorded peak, a small deviation between the measured and fitted signal is observed around the take-off and the apex of the peak. This deviation indicates that the EMG model is not as accurate for the modeling of the extra-column contribution as other, more realistic models may be.

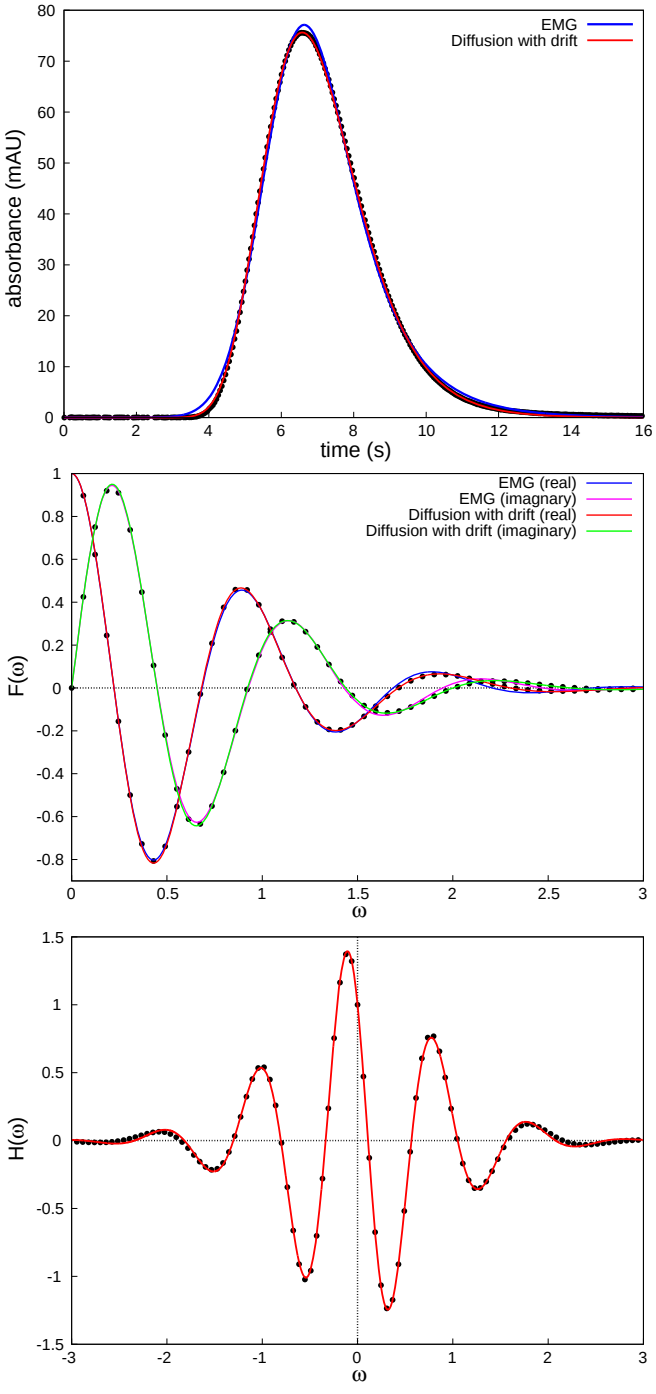

Fig. 1. Curve fitting to the extra-column band profile; the fitting in time domain (top), simultaneous fitting to the real and imaginary parts of the Fourier transform (middle), fitting to the Hartley transform (bottom).

A more accurate model can be formulated by taking the solution of the diffusion equation. Diffusion with drift in a pipe leads to the following first-passage distribution [15]:

$$f(t) = \sqrt{\frac{N_d t_0}{2\pi t^3}}\ \exp\left[-\frac{N_d}{2}\frac{(t-t_0)^2}{t_0 t}\right] \tag{15}$$

where t_0 is the void time and N_d is the plate number due to mobile phase dispersion.

The Fourier transform of $f(t)$ is [15]:

$$F(\omega) = \exp[N_d - \sqrt{N_d(N_d - 2i\omega t_0)}] \tag{16}$$

To consider the mixer-type extra-column volumes, the convolution of Eq. (15) with an exponential decay function

$$f(t) = \frac{e^{-t/\tau}}{\tau} \tag{17}$$

is necessary. The evaluation of that convolution in time domain is rather cumbersome. In Fourier domain, however, convolution can simply be calculated by a multiplication (see Eq. (7)).

The Fourier transform of the exponential decay function is

$$F(\omega) = \frac{1}{1 - i\omega\tau} = \frac{1}{1+\omega^2\tau^2} + i\frac{\omega\tau}{1+\omega^2\tau^2} \tag{18}$$

When we combine the Gaussian and the mixer-type extra-column contributions in Fourier domain, we take the products of Eqs. (16) and (18):

$$F(\omega) = \frac{\exp[N_d - \sqrt{N_d(N_d - 2i\omega t_0)}]}{1 - i\omega\tau} \tag{19}$$

Eq. (19) cannot simply be transformed back to time domain, therefore the direct parameter estimation in time domain is not feasible. On the basis of Eq. (19), the parameter estimation in Fourier or Hartley domain can be carried. out. See Fig. 2b and c and Table 1 for the results of the fitting.

The parameters obtained by fitting Eq. (19), allow the evaluation of the extra-column properties of the instrument. From the value of the first statistical moment, $\mu_1 = t_0 + \tau$, we obtain the extra column volume as $V_{ex} = 59.1$ μL. Its variance is calculated from the second central moment: $\mu'_2 = t_0^2/N_d + \tau^2 = 2.19\ s^2$, which is equivalent to 152.2 μL^2, i.e. the standard deviation due to extra-column broadening is $\sigma = 12.3$ μL.

Although Eq. (19) gives a more accurate model of the extra-column broadening than the EMG function, the numerical values in Table 1 demonstrate that the EMG model can also be utilized for a rough estimation of the peak shape parameters.

4.2. Peak shape of the unretained marker

The peak shape of the injected thiourea was evaluated by means of the peak shape models used in the previous section. The EMG model was fitted in time domain, as well as to the Fourier and Hartley transformed signal. The results are summarized in Fig. 2 and in Table 1. Both the EMG model and the model formulated by combining the diffusion equation with the exponential term fit the observed peak equally.

When peak tailing is due to extra column effects, the EMG model is quite often used to model the peak shape.

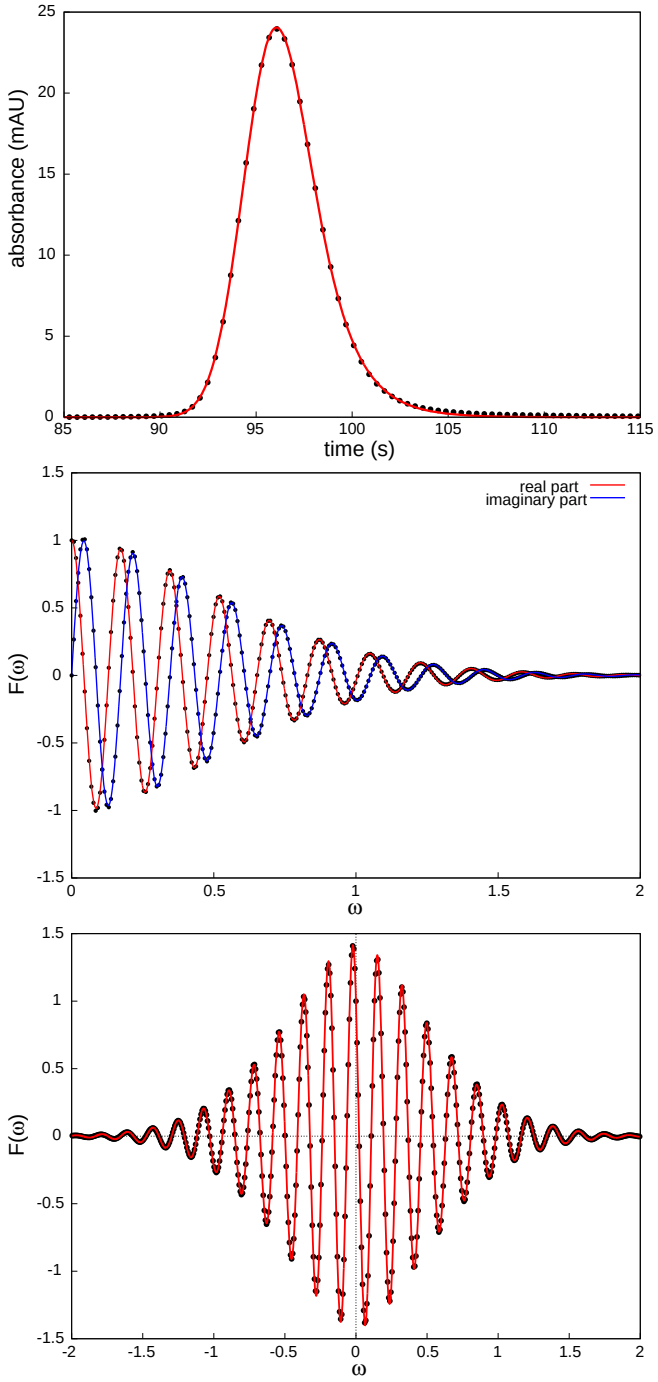

Fig. 2. Curve fitting to the unretained tracer; the fitting in time domain (top), simultaneous fitting to the real and imaginary parts of the Fourier transform (middle), fitting to the Hartley transform (bottom).

4.3. Peak shape of a retained analyte

The peak of phenol – detected in a reversed phase separation system – is plotted in Fig. 3. The peak is fairly symmetrical due to homogeneous interactions between the stationary phase and the solute molecules, but still it carries some asymmetry due to extra/column effects. Again, the EMG model was fitted in time domain, as well as in the Fourier and Hartley domains. The numerical results are summarized in Table 1.

Table 1
Best-fitting peak shape parameters for the instances presented in Figs. 1–3.

	Time domain		Fourier domain		Hartley domain	
Extra-column contribution						
EMG						
m [s] (RSD %)	5.844	(0.088)	5.848	(0.384)	5.841	(0.159)
σ [s] (RSD %)	0.939	(0.464)	0.940	(0.384)	0.939	(0.906)
τ [s] (RSD %)	1.290	(0.750)	1.260	(3.220)	1.275	(1.320)
Diffusion + exponential decay						
N_d (RSD %)	–	–	32.23	(1.41)	–	–
t_0 [s] (RSD %)	–	–	6.074	(0.229)	–	–
τ [s] (RSD %)	–	–	1.023	(1.83)	–	–
Unretained tracer						
EMG						
m [s] (RSD %)	94.99	(0.071)	94.91	(0.097)	94.86	(0.105)
σ [s] (RSD %)	1.461	(0.338)	1.460	(0.183)	1.459	(0.206)
τ [s] (RSD %)	1.601	(0.714)	1.542	(0.360)	1.642	(0.374)
Diffusion + exponential decay						
N_d (RSD %)	–	–	4162	(0.415)	–	–
t_0 [s] (RSD %)	–	–	94.94	(0.0044)	–	–
τ [s] (RSD %)	–	–	1.515	(0.437)	–	–
Phenol						
EMG						
m [s] (RSD %)	658.5	(0.040)	657.9	(0.176)	657.9	(0.179)
σ [s] (RSD %)	6.224	(0.140)	6.207	(0.048)	6.206	(0.792)
τ [s] (RSD %)	2.610	(1.20)	3.272	(3.97)	3.282	(4.02)
Stochastic–dispersive model						
n (RSD %)	–	–	14,933	(0.656)	–	–
τ_s [s] (RSD %)	–	–	0.0378	(0.326)	–	–

Although we can see in Fig. 3 that the EMG model rather nicely fits the peak shape of phenol, here we face a general problem. The EMG model loses its physical meaning when a retained peak is studied. If one wants to gain insights into the details of the separation problem, a real physical model should be employed.

The stochastic model of chromatography offers a rather attractive solution in this instance [16]. This model assumes that while migrating along the column, a molecule performs a random number of adsorption and desorption steps characterized by a Poisson distribution. Furthermore, once a molecule is adsorbed on the stationary phase, the time spent until desorption – the sojourn time – is a random variable, too. This latter random variable follows an exponential distribution. When this model is combined with mobile phase dispersion, the stochastic–dispersive model is obtained [15,17]. The Fourier transform of the peak shape model is

$$\phi_R(\omega) = \exp\left[N_d\left(1 - \sqrt{1 - \frac{2i\omega}{N_d}\left(\frac{n\tau_s}{1 - i\omega\tau_s} + t_0\right)}\right)\right] \tag{20}$$

where n is the mean number of mass transfer steps, τ_s is the average adsorption time, t_0 is the void time, and N_d is the plate number due to mobile phase dispersion. Eq. (20) is the characteristic function of the probability density function of the elution time of the individual molecules. Formally, the characteristic function is identical to the Fourier transform [18].

Since the stochastic model has an analytical solution in the Fourier domain, and only numerical solution in time domain, again, it is convenient to perform the fitting in the Fourier domain. The important numerical values are reported in Table 1. The results show that as the phenol molecules migrate along the column, a single molecule, on the average, adsorbs $n = 14,933$ times, the average adsorption time being $\tau_s = 37.8$ ms.

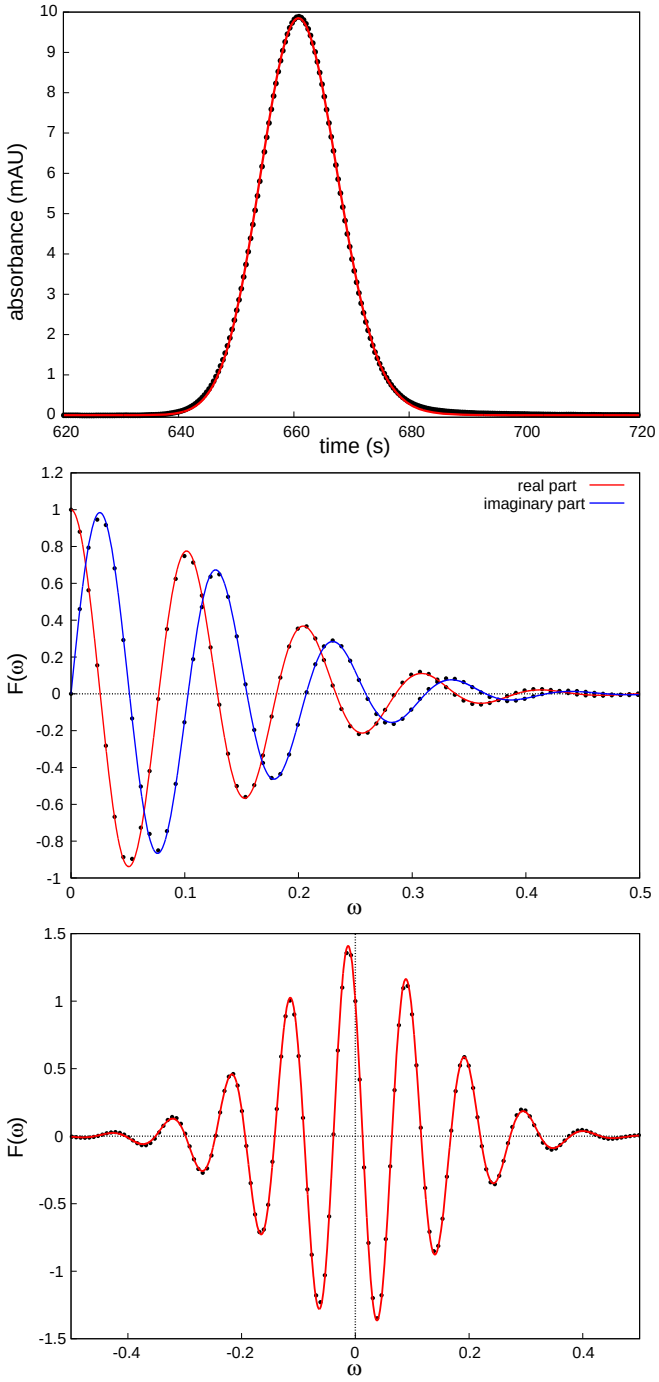

Fig. 3. Curve fitting to the phenol peak; the fitting in time domain (top), simultaneous fitting to the real and imaginary parts of the Fourier transform (middle), fitting to the Hartley transform (bottom).

5. Conclusions

The physical models of flow systems or chromatography are often solved in Fourier of Laplace domain in closed form. The Fourier or Hartley transform of the experimentally recorded signals can be calculated, and the models can directly be fitted. In this case, information from the entire peak shape is utilized.

We have shown using various models of extra-column broadening the importance of the exact physical model. Also the stochastic model of chromatography is rather convenient to fit in the Fourier domain, since the characteristic function of the peak shape is expressed analytically.

The parameter estimation in frequency domain gives results identical to the time domain curve fitting; the accuracy of the frequency domain estimation is excellent. One observes, however, that the precision of the parameter estimation is somewhat worse in frequency domain. That occurs in spite of the fact that Fourier transform separates the low-frequency signal and the high-frequency noise. The noise pattern of the UV detector signals exhibits a brown ($1/f^2$) or pink ($1/f$) spectrum [19]. Thus, the low-frequency component of the noise is more dominant than the high-frequency one and it overlaps with the low-frequency signal in the Fourier or Hartley domain, affecting the precision of the parameter estimation.

Acknowledgments

The work was supported by grants OTKA-NKTH NI-68863, OTKA-K75717.

References

[1] A. Felinger, Data Analysis and Signal Processing in Chromatography, Elsevier, Amsterdam, 1998.
[2] A. Felinger, T.L. Pap, J. Inczédy, Anal. Chim. Acta 248 (1991) 441–446.
[3] N.A. Wright, D.C. Villalanti, M.F. Burke, Anal. Chem. 54 (11) (1982) 1735–1738.
[4] T.A. Maldacker, J.E. Davis, L.B. Rogers, Anal. Chem. 46 (6) (1974) 637–642.
[5] A. Felinger, Anal. Chem. 66 (19) (1994) 3066–3072.
[6] A. Felinger, L. Pasti, F. Dondi, Anal. Chem. 62 (17) (1990) 1846–1853.
[7] A. Felinger, L. Pasti, P. Reschiglian, F. Dondi, Anal. Chem. 62 (17) (1990) 1854–1860.
[8] A. Felinger, L. Pasti, F. Dondi, Anal. Chem. 63 (22) (1991) 2627–2633.
[9] A. Felinger, L. Pasti, F. Dondi, Anal. Chem. 64 (18) (1992) 2164–2174.
[10] F. Dondi, A. Betti, L. Pasti, M.C. Pietrogrande, A. Felinger, Anal. Chem. 65 (17) (1993) 2209–2222.
[11] A. Felinger, T. Pap, J. Inczédy, Talanta 41 (7) (1994) 1119–1126.
[12] L. Hong, A. Felinger, K. Kaczmarski, G. Guiochon, Chem. Eng. Sci. 59 (2004) 3399.
[13] R.N. Bracewell, The Hartley Transform, Oxford Univerrsity Press, New York, 1986.
[14] A. Economou, P.R. Fielden, A.J. Packham, Analyst 121 (1996) 1015–1018.
[15] A. Felinger, A. Cavazzini, F. Dondi, J. Chromatogr. A 1043 (2004) 149.
[16] A. Felinger, J. Chromatogr. A 1184 (2008) 20–41.
[17] A. Felinger, A. Cavazzini, M. Remelli, F. Dondi, Anal. Chem. 71 (1999) 4472–4479.
[18] H. Cramér, Random Variables and Probability Distributions, Cambridge University Press, Cambridge, 1970.
[19] A. Felinger, M. Káré, Chemometr. Intell. Lab. Syst. 72 (2004) 225.